Floquet Engineering in Quantum Chains

D. M. Kennes,[1] A. de la Torre,[2,3] A. Ron,[2,3] D. Hsieh,[2,3] and A. J. Millis[1,4]

[1]*Department of Physics, Columbia University, New York, New York 10027, USA*
[2]*Department of Physics, California Institute of Technology, Pasadena, California 91125, USA*
[3]*Institute for Quantum Information and Matter, California Institute of Technology, Pasadena, California 91125, USA*
[4]*Center for Computational Quantum Physics, The Flatiron Institute, New York, New York 10010, USA*

We consider a one-dimensional interacting spinless fermion model, which displays the well-known Luttinger liquid (LL) to charge density wave (CDW) transition as a function of the ratio between the strength of the interaction U and the hopping J. We subject this system to a spatially uniform drive which is ramped up over a finite time interval and becomes time periodic in the long-time limit. We show that by using a density matrix renormalization group approach formulated for infinite system sizes, we can access the large-time limit even when the drive induces finite heating. When both the initial and long-time states are in the gapless (LL) phase, the final state has power-law correlations for all ramp speeds. However, when the initial and final state are gapped (CDW phase), we find a pseudothermal state with an effective temperature that depends on the ramp rate, both for the Magnus regime in which the drive frequency is very large compared to other scales in the system and in the opposite limit where the drive frequency is less than the gap. Remarkably, quantum defects (instantons) appear when the drive tunes the system through the quantum critical point, in a realization of the Kibble-Zurek mechanism.

The manipulation of materials properties by controlled application of high amplitude electromagnetic fields, with the ultimate goal of creating "quantum matter on demand," is attracting an increasing amount of attention [1,2]. As technology for generating intense electromagnetic pulses across a broad wavelength spectrum has become available, there is an urgency to understand how to use light to induce phenomena that are inaccessible in thermal equilibrium and study its interaction with complex phases of matter.

A system exposed to a time periodic drive may be described by a "Floquet Hamiltonian" [3] with a discrete time translation invariance. While Floquet systems have been studied extensively in atomic physics [4–8], less attention has been paid to solid-state realizations due to the issue of runaway heating. If the drive period matches an excitation energy in the solid, then an ever increasing number of excitations may be generated, driving the system to the infinite temperature limit. However, if the drive frequency is sufficiently detuned from simple excitation energies, for example, by being very high [9–11] or being well within an excitation gap [12–14], runaway heating only occurs at exponentially long times and there is a well-defined intermediate timescale, typically referred to as the prethermal regime, where heating is negligible. The high frequency limit has the added simplification that a low order Magnus expansion [15] can be employed to describe the driven system in terms of an effectively static Hamiltonian with renormalized parameters [16,17].

Most of the theoretical work on Floquet-like systems has been limited to qualitative analysis, (effectively) noninteracting models or small systems in the long-time limit. Important exceptions include the work of Poletti and Kollath [18], where a one-dimensional Bose-Hubbard model with a drive field ramped slowly up from zero was studied, and that of Mentink, Balzer, and Eckstein [12] and Mendoza-Arenas *et al.* [19], who performed dynamical mean field analyses of the destruction of antiferromagnetism upon application of time periodic fields, and its dependence on ramp speed [20–22], and a general discussion of the Floquet adiabatic theory for different drive parameters [23].

In this Letter we present a comprehensive study of an interacting quantum many-body model driven by electromagnetic radiation which vanishes at large negative times, is periodic at large positive times, and is ramped up at controllable rates. We use a numerically exact density matrix renormalization group (DMRG) method [24–26] that is formulated in the thermodynamic (infinite system size) limit [27–29]. We show that this method allows us to access unprecedentedly long times in the prethermal regime where heating may be neglected. We are interested in the dependence of the properties of this prethermal state on the ramp speed of drive and frequency. We find that the long-time Floquet behavior can be qualitatively understood in terms of equilibrium models with renormalized parameters and a temperature which depends on ramp speed and other factors [30]. Finally, we show that a key feature of the Kibble-Zurek case [31–33], in which the drive tunes the

system across a quantum phase transition, is the appearance of quantal (instanton–anti-instanton) defects. Our results demonstrate the power of time-dependent DMRG to study Floquet engineering in interacting systems.

We consider spinless fermions with a nearest-neighbor interaction described by the following Hamiltonian:

$$H(t) = \sum_j \left[-\frac{J(t)}{2} c_j^\dagger c_{j+1} + \text{H.c.} \right.$$
$$\left. + U\left(n_j - \frac{1}{2}\right)\left(n_{j+1} - \frac{1}{2}\right) \right]. \quad (1)$$

The operators c_i and $c_i^\dagger$ annihilate or create spinless fermions at site i, and $n_i = c_i^\dagger c_i$ is the site occupancy. We concentrate on the case of half filling, with $U > 0$ and (without loss of generality) $J > 0$. The equilibrium phase diagram is shown in Fig 1. We choose $J(t) = J e^{iA(t)}$, with $A(t)$ the vector potential corresponding to a spatially uniform electric field $E = -\partial_t A$ and consider a harmonic drive with frequency Ω which is ramped on over a time interval τ:

$$A(t) = \frac{E_0}{\Omega} \sin(\Omega t) \left[\frac{1}{2} + \frac{1}{2} \tanh\left(\frac{t}{\tau}\right) \right]. \quad (2)$$

We consider two frequency regimes: Magnus, $\Omega \gg J, U$ (we choose $\Omega = 10J$), and subgap, $\Omega < \Delta$ (we choose $U = 16J$ and $\Omega = 0.6U$). Previous work on related models [9–14] suggests that in these regimes a parametrically long intermediate-time regime exists in which heating may be neglected and a steady state may be defined. As such, the long-time physics may be understood in terms of pseudoequilibrium arguments based on Hamiltonians renormalized via an appropriate average over a drive period, effectively moving the system from one point to another in the phase diagram (Fig. 1). In this language we distinguish the bare parameters (without the driving) from the effective ones (with the driving), such as the bare gap Δ and the effective gap Δ^{eff} (both can be obtained by Bethe ansatz using the values of U and the bare hopping J or
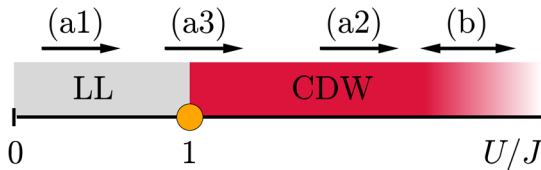

FIG. 1. Ground state phase diagram of Eq. (1) as a function of ratio of interaction strength U to hopping J showing Luttinger liquid (LL) and charge density wave (CDW) phases. Notations (a1)–(a3) and (b) indicate the studied cases, with the direction in which the effective interaction strength can be tuned by a nonequilibrium drive indicated by the arrow head. The circular marker signals the location of the LL to CDW quantum phase transition.

effective hoping J^{eff}, respectively). In the Magnus case it is argued [15] that in the steady state one may simply replace $J(t)$ by its average over a period $2\pi/\Omega$, $J \rightarrow J^{\text{eff}} = J_0(E_0/\Omega)J$. This leads to a decrease in the magnitude of J, because the Bessel function has magnitude less than 1, i.e., an increase in the ratio U/J, implying that the drive moves the system to the right in Fig. 1 as indicated by arrows in the cases (a1)–(a3), either within the Luttinger liquid (LL) phase (a1), within the charge density wave (CDW) phase (a2), or across the quantum critical point separating the two (a3). In the subgap regime, the modification of the Hamiltonian parameters is more involved than in the Magnus case. As noted in Refs. [12,13], if the drive period is small relative to the gap, analytical results may be obtained by retaining only processes that couple adjacent Floquet bands and averaging over a drive period. Applying this method to our model, we find that the long-time behavior may be described by the effective hopping,

$$J^{\text{eff}} = J \sqrt{\sum_{n=-\infty}^{\infty} \left(\frac{J_n(E_0/\Omega)}{1 - n\Omega/U} \right)^2}, \quad (3)$$

which may be either smaller or larger than the starting J, so the system may be moved either to the left or the right on the phase diagram of Fig. 1, but of course only within the gapped phase [Fig. 1, case (b)].

We characterize the out-of-equilibrium behavior via the equal time density-density correlation function C, which depends on relative position j, ramp time τ, and time t:

$$C_{nn}(j, t, \tau) = \left\langle \left(n_0(t) - \frac{1}{2} \right) \left(n_j(t) - \frac{1}{2} \right) \right\rangle, \quad (4)$$

focusing in particular on the t and τ dependence of the large j behavior. In the Luttinger liquid phase at equilibrium as $T \rightarrow 0$, C decays as a power law for large j, while in the CDW phase, C tends exponentially to a nonzero constant. At $T > 0$, C decays exponentially to zero at long scales, with exponent depending on phase, value of interaction, and temperature.

We use the DMRG methods of Refs. [27–29] to solve the model [see Supplemental Material (SM) [34] for details]. We start from the ground state corresponding to $A(t) = 0$ and integrate forward in time. DMRG calculations are limited by the growth of entanglement entropy; in the Magnus and subgap regimes the entanglement remains manageable because there is no runaway heating, allowing us to reach large times. In all cases except the Kibble-Zurek (a3) situation, we find (see the SM [34]) that after times $\sim 100J$ the system reaches a steady state, in which the properties (averaged over a few drive periods) become time independent. We describe the steady state properties by comparing to a pseudothermal state given by a diagonal density matrix.

Figure 2 shows the long-time behavior of C, as a function of inverse ramp time for different distances j.
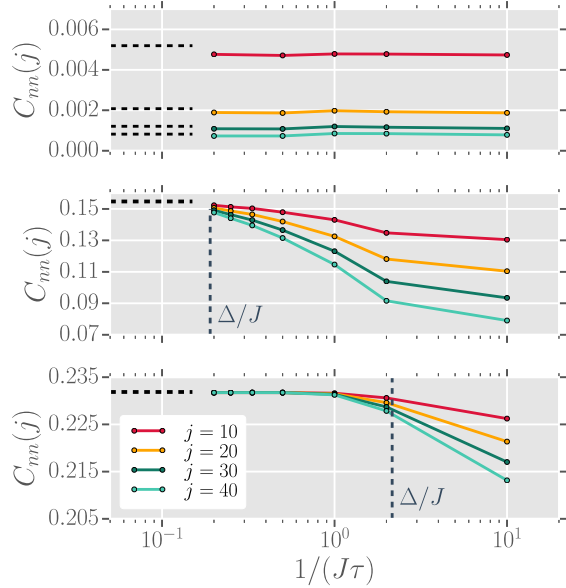
FIG. 2. Density-density correlation function $C(j)$ averaged over the time range $t = 100/J$ to $t = 400/J$ for different j (solid lines) as function of inverse of ramp time τ for $\Omega/J = 10$, $E_0/\Omega = 1$, and $T/J = 0$ (Magnus limit). Top: Initial correlation strength $U/J = 0.5$ (LL phase), Magnus estimate of final correlation strength $U/J_{\rm eff} \approx 0.65$. Middle: Initial state $U/J = 1.75$ (CDW), final $U/J_{\rm eff} \approx 2.29$ (CDW). Bottom: Initial state $U/J = 4$ (CDW), final $U/J_{\rm eff} \approx 5.23$ (CDW). The ground state expectation values from the effective Hamiltonian ($J \to J^{\rm eff}$) are given as horizontal dashed lines and the gaps $\Delta^{\rm eff}$ as vertical dashed lines.

The upper panel shows that when the system is in the Luttinger liquid phase both before and after the ramp [case (a1)] the behavior is completely independent of the ramp time, and that values of the correlation functions are very close to those predicted by using the Magnus formalism to obtain an effective J and then using equilibrium formulas to calculate the $T = 0$ behavior. As shown in the SM, the exponent characterizing the power-law decay is, within our numerical uncertainty, identical to the Magnus estimate but the prefactor is slightly larger [34]. This $T = 0$-like Luttinger liquid behavior is also seen in the momentum dependences displayed in the SM [34]. Thus, in this case the energy injected by a nonadiabatic ramp does not manifest itself as an effective temperature, even for ramp time as low as $\tau = J/10$ (compare Supplemental Material, Fig. S2 [34]). This finding is consistent with previous reports that the integrability of the system means that quenching of a LL from one time-independent Hamiltonian to another preserves the basic power-law decay [35–38].

The middle and lower panels of Fig. 2 study two examples of the case (a2) where the perturbation is expected to shift the system from one point in the CDW regime to another. We again find that after a transient period $\lesssim 100/J$ the system evolves to a steady state, but in contrast to the LL to LL case, we find strong dependence on the ramp time; note in particular the ramp-speed-dependent
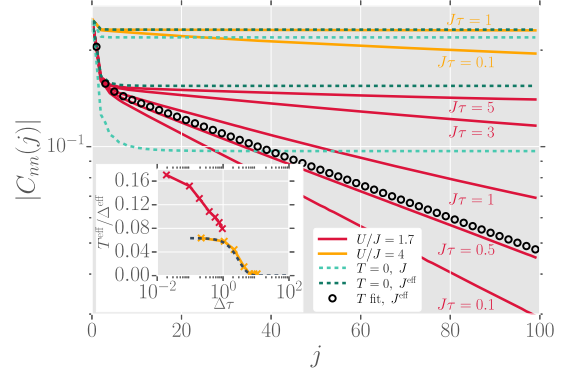

FIG. 3. Main: Time-averaged density-density correlation function $C(j)$ (solid lines) for different $J\tau$ and U/J. The other parameters are $\Omega/J = 10$, $F_0/\Omega = 1$, and $T/J = 0$. The $T = 0$ equilibrium prediction with $J \to J^{\rm eff} = J_0(E_0/\Omega)J$ (dark dashed lines) compares well to the time-averaged results only in the limit of large $J\tau$. The light dashed lines are the undriven equilibrium results. Inset: Effective temperature (crosses) as function of τ extracted by fitting the slope of the exponential tail of the $U/J = 1.7$ and $U/J = 4$ lines in the main panel. One of these fits ($U/J = 1.7$ and $J\tau = 0.5$) of the slope of the exponential tail in j is shown in the main panel by open circles. The approximate prediction $T^{\rm eff}/\Delta^{\rm eff} = a\Delta\tau \sinh(b\tau\Delta)$ is the dashed line (see SM [34]).

exponential decays at large j. Comparison of the two cases indicates that the timescale governing the ramp speed dependence is the inverse of the gap $\Delta^{\rm eff}$ of the final state (obtained from the Bethe ansatz using $J^{\rm eff}$ and U).

Figure 3 considers the case (a2) in more detail, plotting the j dependence of the logarithm of $|C|$ for different ramp speeds and initial correlation strengths. Comparison to the equilibrium behavior suggests that the energy put into the system by a rapid ramp produces an effective temperature $T_{\rm eff}$. The inset shows the effective temperature (see Supplemental Material [34]) defined from $C(j) = C_0 e^{-\Delta^{\rm eff}/T_{\rm eff}}$ (C_0 is the fitting constant). We see that for sufficiently adiabatic ramps, the effective temperature becomes unobservably small, but we believe that for all ramp speeds $T_{\rm eff} \neq 0$. Thus we argue that a nonadiabatic ramp creates a density of defects (as would also be created by a nonzero temperature) which are essentially randomly distributed and do not annihilate over the timescale of our simulations. We finally note that although the long-distance behavior is consistent with a nonzero temperature, the entire j dependence cannot be described with a unique temperature-gap pair. As can be seen from the offset between the open circles and the solid line, the long-distance decay is characterized by a prefactor different from the thermal equilibrium result. Relatedly, the open circles agree very well with the short-time behavior (see SM for more information [34]).

Very similar physics is obtained in the subgap regime [regime (b)]. We find the same dependence on ramp speed
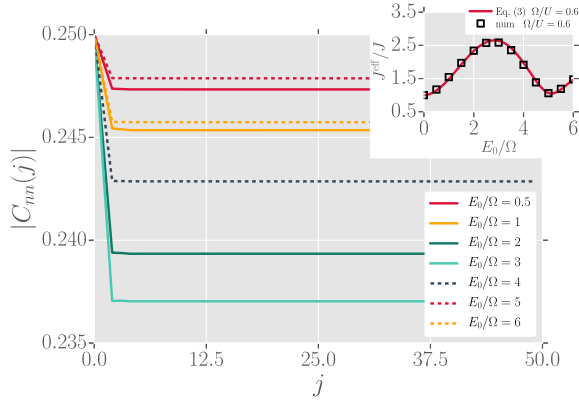
FIG. 4. Main: Time-averaged density-density correlation function $C(j)$ (lines) for different E_0/Ω. The other parameters are $J\tau = 4$, $\Omega/U = 0.6$, $U/J = 16$, and $T/J = 0$. Inset: Comparison of Eq. (3) for effective hopping generated by subgap drive (solid line) and deduced from fits of the data shown in the main panel to the equilibrium $T - 0$ formula for the long-distance limit of C.

as in case (a2). Thus, in Fig. 4 we present only results in the quasiadiabatic limit. For the case considered, the long-time CDW amplitude is smaller than the initial amplitude (drive leads to weaker correlations), but with a nonmonotonic dependence on the ratio of drive strength to frequency. The inset confirms that the $J_{\rm eff}$ obtained by analyzing the data in the main panel agrees perfectly with our theoretical prediction Eq. (3). Remarkably, Eq. (3) describes a highly tunable nonmonotonic control of the ration U/J either to larger or smaller values, which is beyond the control obtained in the Magnus regime (see SM [34]).

We finally show in Fig 5 the case (a3) in which the drive tunes the system across the quantum critical point separating the LL and CDW phases. The $Jt = 20$ [lowest (black)] curve is very similar to the short-time behavior observed in the CDW to CDW quench [cases (a2) and (b)], where C decreases with increasing j. This is qualitatively consistent with a CDW-like phase with amplitude exponentially decaying at large distances. But at slightly longer times ($Jt \sim 25$) a phase-slip–antiphase-slip pair appears: as j is increased, the amplitude goes to zero, and then increases again, but with the opposite phase (maxima in the positions where an extrapolation of the small j curve would predict minima), then the amplitude again goes to zero, and then the oscillations are in phase with the small j ones. The phase slip and antiphase slip separate rapidly in space, then remain at a roughly fixed distance for a time interval $\sim 100/J$ and then recoalesce, leaving a single phase regime (see inset). Such phase-slip–antiphase-slip pairs were not observed in any of our CDW $\to$ CDW cases (see SM [34]). Thus, we interpret the phase-antiphase slip pairs as quantum defects produced in the manner of Kibble and Zurek [31] because the trajectory in parameter space passes close to the quantum critical point.

The first distance at which the phase-slip–antiphase-slip pair appears is somewhat dependent on ramp speed and
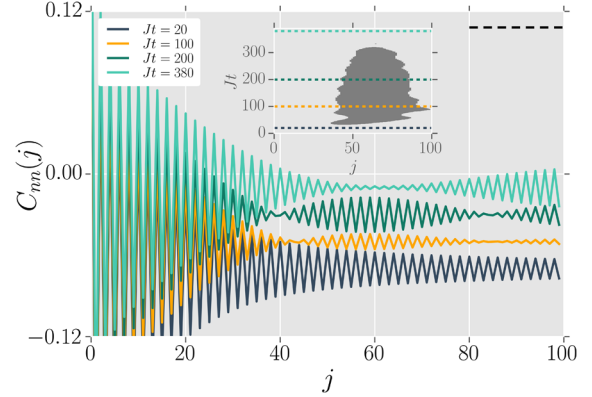

FIG. 5. Main: The correlation function $C(j)$ at different times averaged over one drive period for the Kibble-Zurek (a3) case. Lines are shifted vertically for clarity of depiction; the midpoint of the oscillation is zero. The dashed black line gives the asymptotic value expected at large j from a ground state calculation using the Magnus formalism, shifted to correspond to the longest time case. Inset: Time evolution of the phase averaged over the drive period. Light and dark gray denote the phase of $C + 1$ and -1 with respect to the small j oscillation, respectively. The parameters are $U/J = 0.95$, $E_0/\Omega = 1.5$, $J\tau = 4$, and $T/J = 0$.

drive strength, as is the time over which the phase slip and antiphase slip exist, but in all cases we have investigated the first time at which the pair appears is about the same ($Jt \sim 30$). The relatively weak dependence of many of the phase-slip properties on parameters (see SM [34]) may be related to the logarithmic scaling associated with the Kosterlitz-Thouless-like criticality of the model at $U = J$. Note that unlike the defects which give rise to the exponential decay, these instantons anneal out in a finite time.

In summary, this Letter has established DMRG as an efficient tool to study Floquet engineering in interacting quantum systems in situations where heating can be neglected over a wide time range. In this wide time range, it is generally accepted [9–14] that the system is in a "prethermal" state described by a diagonal density matrix. We investigated three different Floquet engineering cases (LL $\to$ LL, CDW $\to$ CDW, and LL $\to$ CDW), finding three different types of prethermal states. In the LL $\to$ LL case the energy put into the system as the drive is turned on does not manifest itself as an effective temperature. On the other hand, in the CDW $\to$ CDW case the energy does lead to a behavior closely analogous to that found in thermal equilibrium, while the key feature of the LL $\to$ CDW case is an interesting generation of finite lifetime quantal defects if the drive moves the system across a quantum phase transition. We also derived and numerically verified an expression for drive-induced parameter changes that goes beyond the standard Magnus expression and admits a weakening as well as a strengthening of the effective correlation parameter. Our work opens many directions for research.

The methods presented here can be applied to many other one-dimensional situations including ladders, higher-spin and longer-ranged interaction spin chains, and doped systems. This work sets the basis for the study of interacting spinful fermions of relevance to quasi-1D conducting materials such as $Li_{0.9}Mo_6O_{17}$ (purple bronze) [39], the organic salt TTF-TCNQ [40], or $NbSe_3$ [41]. $NbSe_3$ in particular may be particularly amenable to Floquet engineering because its CDW gap scale is in the midinfrared [41], a region readily accessible by modern high pulse-energy lasers.

Other future directions include a study of the effect of pulses of finite duration. On the analytic side, an improved understanding of the LL $\rightarrow$ CDW quench is urgently needed.

[1] D. N. Basov, R. D. Averitt, and D. Hsieh, Nat. Mater. **16**, 1077 (2017).

[2] R. Mankowsky, M. Forst, and A. Cavalleri, Rep. Prog. Phys. **79**, 064503 (2016).

[3] J. H. Shirley, Phys. Rev. **138**, B979 (1965).

[4] C. Cohen-Tannoudji, J. Dupont-Roc, and G. Grynberg, *Atom-Photon Interactions* (Wiley Interscience, Chichester, England, 1998).

[5] A. Eckardt, C. Weiss, and M. Holthaus, Phys. Rev. Lett. **95**, 260404 (2005).

[6] A. Zenesini, H. Lignier, D. Ciampini, O. Morsch, and E. Arimondo, Phys. Rev. Lett. **102**, 100403 (2009).

[7] A. P. Itin and M. I. Katsnelson, Phys. Rev. Lett. **115**, 075301 (2015).

[8] F. Meinert, M. J. Mark, K. Lauber, A. J. Daley, and H.-C. Nägerl, Phys. Rev. Lett. **116**, 205301 (2016).

[9] D. A. Abanin, W. De Roeck, and F. Huveneers, Phys. Rev. Lett. **115**, 256803 (2015).

[10] T. Mori, T. Kuwahara, and K. Saito, Phys. Rev. Lett. **116**, 120401 (2016).

[11] T. Kuwahara, T. Mori, and K. Saito, Ann. Phys. (Amsterdam) **367**, 96 (2016).

[12] J. H. Mentink, K. Balzer, and M. Eckstein, Nat. Commun. **6**, 6708 (2015).

[13] M. Claassen, H.-C. Jiang, B. Moritz, and T. P. Devereaux, Nat. Commun. **8**, 1192 (2017).

[14] F. Peronaci, M. Schiró, and O. Parcollet, arXiv:1711.07889.

[15] W. Magnus, Commun. Pure Appl. Math. **7**, 649 (1954).

[16] M. Bukov, L. D'Alessio, and A, Adv. Phys. **64**, 139 (2015).

[17] M. Bukov, M. Kolodrubetz, and A. Polkovnikov, Phys. Rev. Lett. **116**, 125301 (2016).

[18] D. Poletti and C. Kollath, Phys. Rev. A **84**, 013615 (2011).

[19] J. J. Mendoza-Arenas, F. J. Gomez-Ruiz, M. Eckstein, D. Jaksch, and S. R. Clark, Ann. Phys. (Berlin) **529**, 1700024 (2017).

[20] N. Eurich, M. Eckstein, and P. Werner, Phys. Rev. B **83**, 155122 (2011).

[21] A. Herrmann, Y. Murakami, M. Eckstein, and P. Werner, Europhys. Lett. **120**, 57001 (2017).

[22] M. Schüler, Y. Murakami, and P. Werner, arXiv:1712 .06098.

[23] P. Weinberg, M. Bukov, L. D'Alessio, A. Polkovnikov, S. Vajna, and M. Kolodrubetz, Phys. Rep. **688**, 1 (2017).

[24] S. R. White, Phys. Rev. Lett. **69**, 2863 (1992).

[25] G. Vidal, Phys. Rev. Lett. **98**, 070201 (2007).

[26] U. Schollwöck, Ann. Phys. (Amsterdam) **326**, 96 (2011).

[27] C. Karrasch and J. E. Moore, Phys. Rev. B **86**, 155156 (2012).

[28] T Barthel, New J. Phys. **15**, 073010 (2013).

[29] D. M. Kennes and C. Karrasch, Comput. Phys. Commun. **200**, 37 (2016).

[30] S. Lorenzo, J. Marino, F. Plastina, G. M. Palma, and T. J. G. Apollaro, Sci. Rep. **7**, 5672 (2017).

[31] T. W. B. Kibble, J. Phys. A **9**, 1387 (1976); Phys. Rep. **67**, 183 (1980); W. H. Zurek, Nature (London) **317**, 505 (1985); Acta Phys. Pol. B **24**, 1301 (1993); Phys. Rep. **276**, 177 (1996).

[32] S. R. Manmana, S. Wessel, R. M. Noack, and A. Muramatsu, Phys. Rev. B **79**, 155104 (2009).

[33] B. Gardas, J. Dziarmaga, and W. H. Zurek, Phys. Rev. B **95**, 104306 (2017).

[34] See Supplemental Material at http://link.aps.org/supplemental/10.1103/PhysRevLett.120.127601 for discusses further numerical details as well as the details about the occurrence and dynamics of phase slip.

[35] M. A. Cazalilla, Phys. Rev. Lett. **97**, 156403 (2006).

[36] J. Rentrop, D Schuricht, and V Meden, New J. Phys. **14**, 075001 (2012).

[37] D. M. Kennes and V. Meden, Phys. Rev. B **88**, 165131 (2013).

[38] Aditi Mitra, Phys. Rev. B **87**, 205109 (2013).

[39] C. Schlenker, H. Schwenk, C. Escribe-Filippini, and J. Marcus, Physica (Amsterdam) **135**, 511 (1985).

[40] D. Jérome and H. Schulz, Adv. Phys. **31**, 299 (1982).

[41] H. Haifeng and Z. Dianlin, Phys. Rev. Lett. **82**, 811 (1999).